Iron in ice cores from Law Dome: A record of atmospheric iron deposition for maritime East Antarctica during the Holocene and Last Glacial Maximum

Ross Edwards, Peter Sedwick, Vin Morgan, Claude F. Boutron

Geochemistry Geophysics Geosystems G3
AN ELECTRONIC JOURNAL OF THE EARTH SCIENCES
Published by AGU and the Geochemical Society

Research Letter
Volume 7, Number 12
1 December 2006
Q12Q01, doi:10.1029/2006GC001307
ISSN: 1525-2027

Iron in ice cores from Law Dome: A record of atmospheric iron deposition for maritime East Antarctica during the Holocene and Last Glacial Maximum

Ross Edwards
Desert Research Institute, 2215 Raggio Parkway, Reno, Nevada 89512, USA (redwards@dri.edu)

Peter Sedwick
Bermuda Biological Station for Research, Ferry Reach, St. George's, GE01, Bermuda

Institute of Antarctic and Southern Ocean Studies, University of Tasmania, Hobart, Tasmania, Australia

Vin Morgan
Antarctic Climate and Ecosystems Cooperative Research Center, Box 252-80, Hobart, Tasmania 7001, Australia

Australian Antarctic Division, Kingston, Tasmania, Australia

Claude Boutron
Laboratoire de Glaciologie et Géophysique de l'Environnement du CNRS, 54 Rue Molière, F-38402 St. Martin d'Hères Cedex, France

[1] Total dissolvable iron (TDFe) was measured in sections of ice cores recovered from Law Dome on the coast of Wilkes Land, East Antarctica. These samples include ice dating from the Last Glacial Maximum (LGM), the Last Deglaciation, and the early and mid Holocene as well as samples from the Anthropocene that have been dated with seasonal to annual resolution. Combining our TDFe concentration data with estimates of the ice accumulation rate, we estimate the atmospheric iron deposition for Law Dome and the adjacent Southern Ocean during these periods. Our results indicate that the atmospheric iron deposition flux to this region during the LGM ($\sim$8 μmol Fe m^{-2} yr^{-1}) was an order of magnitude higher than the average Holocene deposition flux ($\sim$0.8 μmol Fe m^{-2} yr^{-1}). This Holocene flux estimate is significantly higher than recent estimates of atmospheric iron deposition based on the analysis of iron in samples of the Dome C EPICA ice core, implying that there are significant meridional gradients in eolian iron flux to the Antarctic region. Our data also suggest that there have been significant variations in atmospheric iron deposition to Law Dome and adjacent ocean waters over seasonal to decadal timescales during the past century. Analysis of ice samples dating from calendar years 1927 to 1928 indicates an anomalously high flux of TDFe to the Law Dome region, amounting to around half the maximum LGM flux, possibly as a result of severe drought conditions on the Australian continent. Given that chronic iron deficiency is thought to limit phytoplankton production in much of the ocean around Antarctica, such large secular variations in atmospheric iron supply are likely to have had profound impacts on year-to-year primary production and ecosystem structure in Antarctic waters.

Components: 8777 words, 7 figures, 4 tables.

Keywords: atmospheric iron deposition; Antarctica; Southern Ocean; Last Glacial Maximum.

Index Terms: 0414 Biogeosciences: Biogeochemical cycles, processes, and modeling (0412, 0793, 1615, 4805, 4912); 0315 Atmospheric Composition and Structure: Biosphere/atmosphere interactions (0426, 1610); 0714 Cryosphere: Clathrate.

Received 15 March 2006; **Revised** 28 August 2006; **Accepted** 11 September 2006; **Published** 1 December 2006.

Edwards, R., P. Sedwick, V. Morgan, and C. Boutron (2006), Iron in ice cores from Law Dome: A record of atmospheric iron deposition for maritime East Antarctica during the Holocene and Last Glacial Maximum, *Geochem. Geophys. Geosyst.*, *7*, Q12Q01, doi:10.1029/2006GC001307.

Theme: Eolian Dust as a Player and Recorder of Environmental Change
Guest Editors: Jan-Berend Stuut, Maarten Prins, and Denis-Didier Roussseau

1. Introduction

1.1. Significance of Atmospheric Iron Deposition to the Southern Ocean

[2] The availability of iron (Fe) is known to limit the growth rate and biomass of phytoplankton over much of the modern-day Southern Ocean [*Martin et al.*, 1990; *Boyd et al.*, 2000; *Coale et al.*, 2004; *de Baar et al.*, 2005]. This vast circumpolar region has extremely low surface water Fe concentrations and receives the lowest atmospheric Fe input of the world's oceans [*Duce and Tindale*, 1991; *Jickells et al.*, 2005]. The low concentrations of iron that are available to phytoplankton in surface waters of the present-day Southern Ocean surface are largely supplied by the upwelling of deeper waters [*de Baar et al.*, 1995; *Fung et al.*, 2000; *Watson et al.*, 2000]. However, the transport of iron-bearing dust to the oceans is thought to have been much greater during glacial periods of the late Quaternary, which may have enhanced the supply of biologically available iron to the Southern Ocean during those times [*De Angelis et al.*, 1987; *Martin*, 1990; *Petit et al.*, 1999; *Mahowald et al.*, 1999; *Ridgwell and Watson*, 2002; *Wolff et al.*, 2006]. On the basis of the inverse correlation between atmospheric dust loads and atmospheric CO_2 levels inferred from ice core records, *Martin* [1990] proposed the glacial iron hypothesis, which contends that enhanced atmospheric iron deposition during the last glacial age stimulated oceanic export production, primarily in the Southern Ocean, thus affecting an 80 to 90 ppm decrease in atmospheric CO_2 concentration relative to interglacial conditions.

[3] Major arguments that have been leveled against this hypothesis concern (1) the relative timing of atmospheric dust and CO_2 changes as recorded in ice cores, which indicate significant differences in the timing of decreases in dust deposition versus increases in atmospheric CO_2 at glacial terminations [*Broecker and Henderson*, 1998; *Wolff et al.*, 2006; *Gaspari et al.*, 2006]; (2) the magnitude of atmospheric CO_2 drawdown resulting from plausible increases in Southern Ocean new production, which modeling studies have estimated at less than 10 ppm CO_2 [*Lefèvre and Watson*, 1999; *Popova et al.*, 2000]; and (3) the flux of iron-bearing dust to the ocean during glacial times, which may have been considerably less than that required by Martin's iron hypothesis [*Maher and Dennis*, 2001]. However, more recent modeling studies have simulated a significant drawdown in atmospheric CO_2 (>10 ppm) due to elevated Southern Ocean export production forced by increased iron deposition during glacial times, with the relative timing of simulated changes in atmospheric dust and CO_2 levels in good agreement with ice core records [*Watson et al.*, 2000; *Ridgwell and Watson*, 2002; *Ridgwell et al.*, 2002; *Bopp et al.*, 2003]. Furthermore, increased Si input to the surface ocean and/or changes in the Si:N uptake ratio of phytoplankton due to enhanced iron availability afford additional mechanisms for reducing atmospheric CO_2 during glacial periods, via a decrease in the rain ratio of calcium carbonate to organic carbon [*Brzezinski et al.*, 2002; *Matsumoto et al.*, 2002; *Ridgwell et al.*, 2002].

[4] An important conclusion of these modeling studies is that both the magnitude and timing of simulated glacial-interglacial atmospheric CO_2 changes are highly sensitive to the magnitude and time variation of atmospheric iron deposition to the Southern Ocean. The model simulations of *Watson*

et al. [2000] and *Ridgwell and Watson* [2002] are informed by an atmospheric dust deposition that follows the Vostok ice core dust record [*Petit et al.*, 1999] between maximum (Last Glacial Maximum) and minimum (Holocene) deposition estimates derived from the general circulation dust-transport model of *Mahowald et al.* [1999], with the assumption that the dust contains 3.5% iron by mass of which 2% is readily soluble (i.e., biologically available to marine phytoplankton). The resulting estimates of atmospheric iron deposition contain significant uncertainties, particularly in the model-derived Holocene and Last Glacial Maximum (LGM) dust deposition fluxes, which may significantly overestimate deposition in the Antarctic [*Mahowald et al.*, 1999; *Ridgwell and Watson*, 2002; *Bopp et al.*, 2003], and in the estimated solubility of aerosol iron, which may exceed 10% for dust deposited in and on Antarctic snow [*Edwards and Sedwick*, 2001]. There is thus a pressing need for accurate estimates of the past and present atmospheric deposition of biologically available iron in the Southern Ocean, to evaluate the role of this flux in regulating oceanic algal production and the ocean-atmosphere CO_2 balance.

1.2. Records of Atmospheric Iron Deposition From Antarctic Ice Cores

[5] Model-derived estimates of past and present eolian iron deposition to the Southern Ocean contain large uncertainties [*Tegen and Fung*, 1994; *Mahowald et al.*, 1999, 2005; *Moore et al.*, 2000; *Prospero et al.*, 2002; *Jickells et al.*, 2005], whereas the records of eolian dust derived from deep-sea sediment cores [e.g., *Rea*, 1994; *Kumar et al.*, 1995; *Hesse and McTainsh*, 1999] may be obscured by physical and chemical processes in the water column and sediments. The most reliable estimates of atmospheric iron deposition to the Southern Ocean are likely to be those derived from the analysis of modern and ancient Antarctic snow. Measurements of iron in snow collected from Antarctic pack ice and coastal sites have been used to infer the present-day fluxes and solubility of eolian iron to maritime East Antarctica [*Edwards and Sedwick*, 2001], whereas records of past atmospheric iron deposition have been derived from analysis of aluminum (Al) [*De Angelis et al.*, 1987], dust particles [*Petit et al.*, 1999] or iron [*Edwards et al.*, 1998; *Traversi et al.*, 2004; *Gaspari et al.*, 2006, *Wolff et al.*, 2006] in the ancient snow of Antarctic glacial ice cores. Direct measurements of iron in snow and ice are expected to provide the most robust estimates of eolian iron deposition, because differences in sources and/or atmospheric transport of mineral aerosols can result in variations in Fe/Al or Fe/particle ratios, relative to average crustal values [*Zoller et al.*, 1974; *Arimoto et al.*, 1995; *Holmes and Zoller*, 1996; *Watson*, 1997; *Hinkley and Matsumoto*, 2001; *Jickells and Spokes*, 2001; *Prospero et al.*, 2002; *Bay et al.*, 2004; *Delmonte et al.*, 2004b, 2004c; *Gaspari et al.*, 2006].

[6] *Gaspari et al.* [2006] and *Wolff et al.* [2006] have recently published estimates of eolian iron fluxes for Antarctica spanning the Last Deglaciation (LD) and the last eight glacial cycles, respectively, based on the analysis of iron in the EPICA ice core, which was drilled at Dome C on the inland plateau of East Antarctica. *Gaspari et al.* [2006] estimate that atmospheric deposition of acid-dissolvable iron at the LGM was more than 30-fold higher than during the early Holocene. This recent work represents an important advance in our knowledge of past atmospheric iron deposition to Antarctica, and in our ability to evaluate the impact of changes in atmospheric iron deposition of algal production in the surface ocean. However, it is important to recognize that there may be significant meridional and zonal gradients in the deposition of iron-bearing mineral dust to Antarctica and the Southern Ocean [*Mahowald et al.*, 1999, 2006; *Lunt and Valdes*, 2002; *Delmonte et al.*, 2004a, 2004b]. For example, *Edwards and Sedwick* [2001] reported order-of-magnitude differences in the estimated seasonal deposition fluxes of acid-dissolvable iron between different sectors of maritime East Antarctica, based on the analysis of iron in modern snow samples. Hence ice core records from multiple coastal locations around the Antarctic continent are required to better constrain the past and present atmospheric deposition of iron to the surrounding Southern Ocean.

[7] In this paper, we present results from the analysis of iron in sections of glacial ice cores from Law Dome, in maritime East Antarctica, which extend the preliminary data set presented by *Edwards et al.* [1998]. By combining our iron concentration data with estimates of snow and ice accumulation rates for these core sections, we calculate atmospheric iron deposition fluxes for this location during recent times, the early and late Holocene, the LD, and the LGM. Our data thus provide information on the temporal variability of eolian iron deposition at Law Dome over timescales ranging from seasons to millennia, albeit at rather coarse resolution. Given that this site is

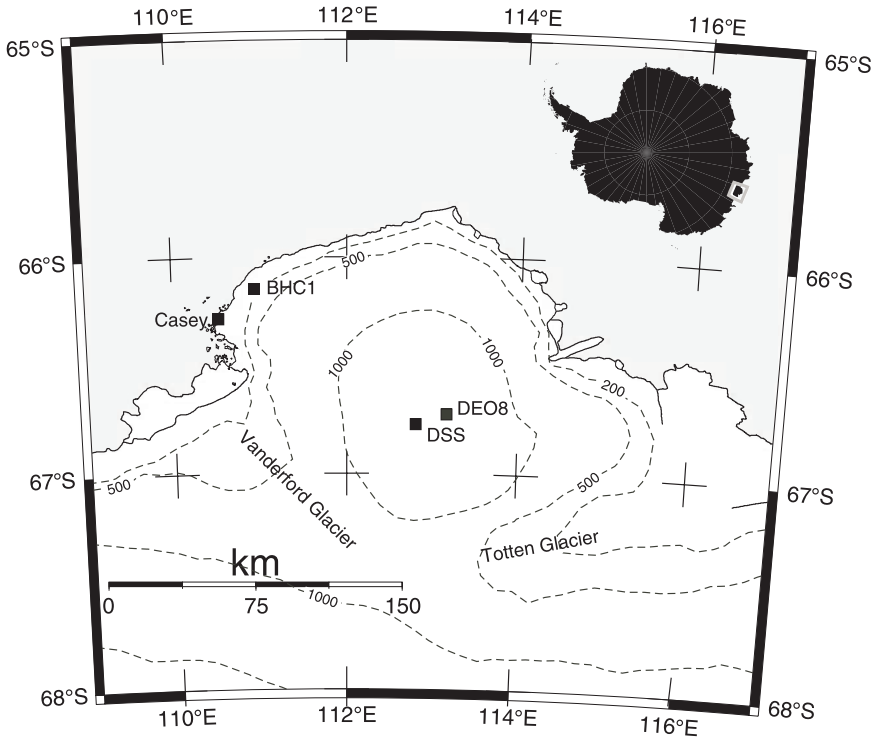

Figure 1. Location map of Law Dome showing locations of ice cores used in this study.

exposed to predominantly maritime atmospheric circulation, these flux estimates are likely to be representative of atmospheric iron deposition over the adjacent polar waters of the Southern Ocean.

2. Ice Cores

2.1. Ice Core Locations

[8] Law Dome is located on the periphery of the East Antarctic ice sheet near the coast of Wilkes Land, East Antarctica (Figure 1). Approximately 200 km in diameter, the Law Dome ice cap has a summit elevation of 1389 m above sea level and a maximum ice thickness of 1200 m [*Hamley et al.*, 1986]. Ice flow from the Law Dome summit is relatively independent of the main East Antarctic ice sheet, which drains into the Totten and Vanderford glaciers, located to the southeast and southwest, respectively (Figure 1). Prevailing easterly winds from the Southern Ocean produce an orographic flow over the ice cap, resulting in high snow accumulation rates (>1 m ice-equivalent per year) on the eastern side and lower rates (<0.5 m ice-equivalent per year) in the west [*Morgan et al.*, 1997]. Here we present results of analyses of sections of three ice cores, DSS, DE08 and BHC1, which were drilled on Law Dome between 1982 and 1993 (Figure 1 and Table 1). For this study, recent and Holocene-age ice samples were

Table 1. Description of Law Dome Ice Cores Used in This Study

Core Site	Location	Average Ice or Snow Accum. Rate, m H_2O equivalent yr^{-1}	Max. Core Depth, m	Time Span of Core, years
DSS	66°46.18′S, 112°48.42′E	0.640[a]	1200	~40,000
DE08	66°43.32′S, 113°11.97′E	1.16[b]	234	~180
BHC1	66°07.83′S, 110°56.28′E	0.06[c]	300	~40,000

[a] *Morgan et al.* [1997].
[b] *Etheridge et al.* [1988].
[c] *Morgan and McCray* [1985].

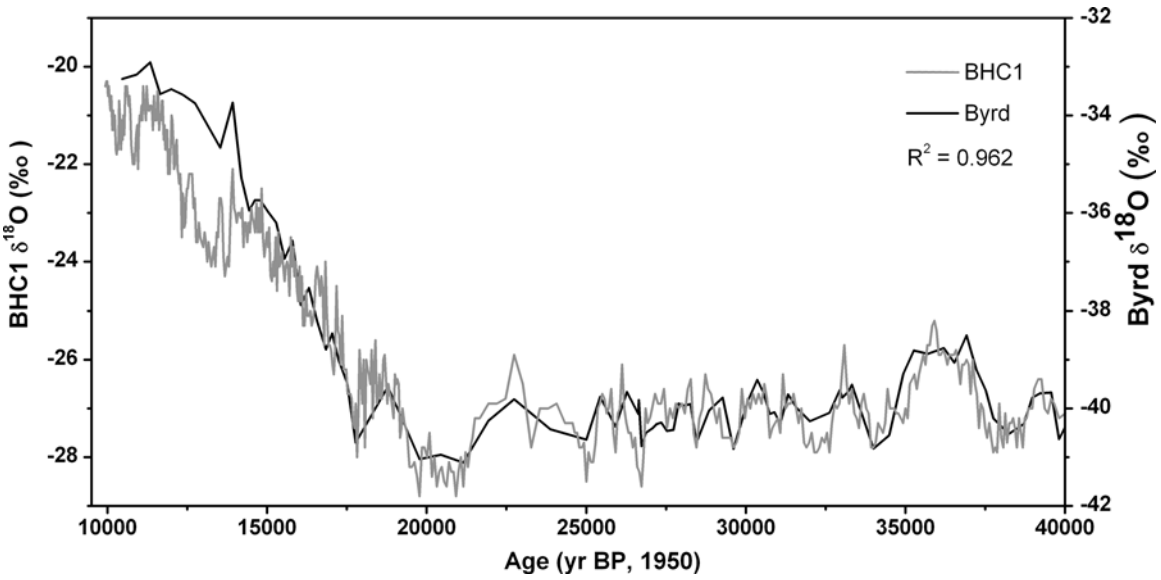

Figure 2. The $\delta^{18}O(H_2O)$ records for the Byrd and BHC1 ice cores [*Blunier and Brook*, 2001, and references therein; *Morgan and McCray*, 1985] mapped on to the GRIP ice core timescale, based on common features in the Byrd and BHC1 down-core records.

selected from sections of cores DSS and DE08, which were recovered from high snow accumulation-rate sites located approximately 18 km apart near the Law Dome summit (Figure 1). Because the oldest sections of these summit cores were highly fractured and thus unsuitable for trace metal analysis, samples dating from the LD and LGM were taken from sections of the BHC1 core, which was drilled near Cape Folger, 109 km northwest of the DSS site (Figure 1). The BHC1 site lies on a flow line running from the Law Dome summit to Cape Folger, along which a series of cores were drilled to study the physical properties of the ice cap [*Etheridge*, 1989; *Morgan and McCray*, 1985; *Russell-Head and Budd*, 1979]. Oxygen isotope data from these cores, together with results of ice-flow modeling and radio echo sounding, indicate that the LGM and LD-age sections of the BHC1 core were originally deposited in the vicinity of the Law Dome summit [*Rowden-Rich and Wilson*, 1996; *Morgan*, 1993; *Etheridge et al.*, 1988].

2.2. Ice Core Chronology

[9] The DE08 core chronology was constrained by counting annual layers determined from the seasonal variations in $\delta^{18}O(H_2O)$ [*Etheridge et al.*, 1988]. The age-depth relationship for the DSS core was determined using several methods, including (1) locating known volcanic horizons and counting of annual layers using seasonal variations of $\delta^{18}O(H_2O)$, hydrogen peroxide, sulfate and conductivity for the Holocene period; (2) gas concentrations synchronized to the Byrd-GRIP timescale of *Blunier and Brook* [2001]; and (3) a flow-thinning model for the oldest core sections [*Morgan et al.*, 2002]. For the LD and LGM age sections of core BHC1, our age-depth chronology is based on comparison of the BHC1 and Byrd-GRIP ice core $\delta^{18}O$ records (Figure 2), using the Analyseries software (lineage tool) to map the Byrd-GRIP timescale on to the BHC1 isotope record ($r^2 = 0.955$).

3. Methods

[10] Subsamples were taken from the ice core sections as described by *Edwards et al.* [1998] and decontaminated by the method of *Candelone et al.* [1994], using stringent trace metal clean procedures to remove contaminated outer layers of the ice core sections. Detailed descriptions of the decontamination procedures are given by *Edwards* [2000] and *Edwards et al.* [1998]. The decontaminated ice core samples were melted and acidified to ~pH 1.9 by addition of Seastar ultrapure concentrated hydrochloric acid (to 0.1% by volume concentrated acid), and then stored at room temperature in acid-cleaned Nalgene low-density polyethylene bottles for more than three months, to allow for dissolution of the "acid-labile" iron-bearing mineral particles. This minimum storage

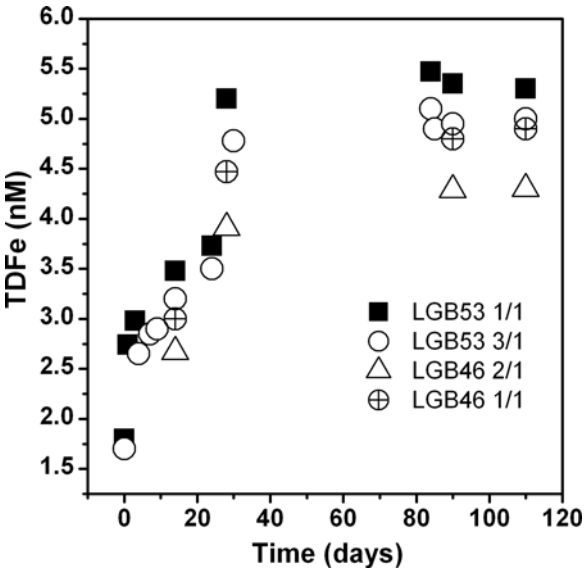

Figure 3. Measured TDFe concentration in acidified Antarctic snowmelt waters as a function of time after acidification from *Edwards* [2000] (see text). A number of deionized-water blanks were analyzed alongside the samples; TDFe remained below the detection limit (~0.3 nM) in all of the blanks.

time was based on the results of repeated analyses of acidified Antarctic snowmelt waters over a period of four to five months, which demonstrate a significant increase in measured iron concentrations for up to three months following acidification to pH 1.9 with hydrochloric acid (Figure 3) [*Edwards*, 2000; *Edwards and Sedwick*, 2001]. We define the fraction of iron that we measure in solution after more than three months storage at pH 1.9 as "total-dissolvable iron." As discussed by *Edwards and Sedwick* [2001], most of the iron contained in polar snow and ice samples is thought to be rendered soluble under mildly acidic conditions, with the exception of that contained within the lattice of highly refractory aluminosilicate particles. The latter is unlikely to enter into the oceanic iron cycle, and is thus of little relevance with regard to the glacial iron hypothesis. The total-dissolvable iron concentrations presented in this paper can be considered as a firm upper limit on the eolian iron that is potentially available to phytoplankton in the surface ocean.

[11] Total-dissolvable iron (TDFe) was determined in the acidified meltwaters by flow injection analysis (FIA) using a modification of the method of *Measures et al.* [1995], which is further detailed by *Bowie et al.* [2004] and *Sedwick et al.* [2005], without sample preconcentration. The accuracy of the FIA measurements was verified by reanalysis of meltwater samples using high-resolution inductively coupled plasma mass spectrometry (ICP-MS) [*Townsend and Edwards*, 1998; *Edwards*, 2000].

4. Results and Discussion

4.1. Iron Concentrations

[12] The TDFe concentrations of all ice core samples analyzed in this study are presented in Figure 4 and Table 2. In samples dating from the past 200 yr (also known as the Anthropocene [*Crutzen and Stoermer*, 2000]), the meltwater TDFe concentrations range from 0.5 nM to 6.0 nM, with considerable variability evident on seasonal to decadal timescales (Figure 5). These TDFe concentrations are generally lower than values we have measured in modern Antarctic snow, with the exception of snow samples collected from the seasonal sea ice zone to the northeast of Law Dome [*Edwards and Sedwick*, 2001]. Several of these ice samples do not integrate a full year, due to the high snow-accumulation rates at the DSS and DE08 sites (Table 2) and the maximum sample size that can be accommodated during the decontamination procedure. The results for these samples suggest that there may be seasonal variations of as much as a factor of 4 in atmospheric iron deposition, with the highest TDFe concentrations measured in core sections dating from the austral summer and autumn. The highest TDFe concentrations in the Anthropocene samples were measured in sections of core DE08 dating from calendar years 1927 to 1928 (Figure 5); the TDFe concentrations in these samples (~4.5–6 nM) were as much as five times higher than the average TDFe concentration (1.2 nM) of all remaining Holocene-age ice samples.

[13] We note that the late 1920s were marked by drought conditions across much of southeastern Australia [*Dai et al.*, 1998, 2004], particularly in South Australia, which experienced severe land degradation due to overgrazing [*Donovan*, 1995]. In addition, red dust was observed in New Zealand snow in 1928 (P. Marshall and E. Kidson, cited by *Warren and Wiscombe* [1980]), indicating the transport of significant quantities of Australian dust across the Tasman Sea and presumably into the Southern Ocean. When considered together with our ice core TDFe data, these observations imply that the Australian continent has been an important source of mineral dust to maritime East Antarctica during the recent past. This suggestion is supported

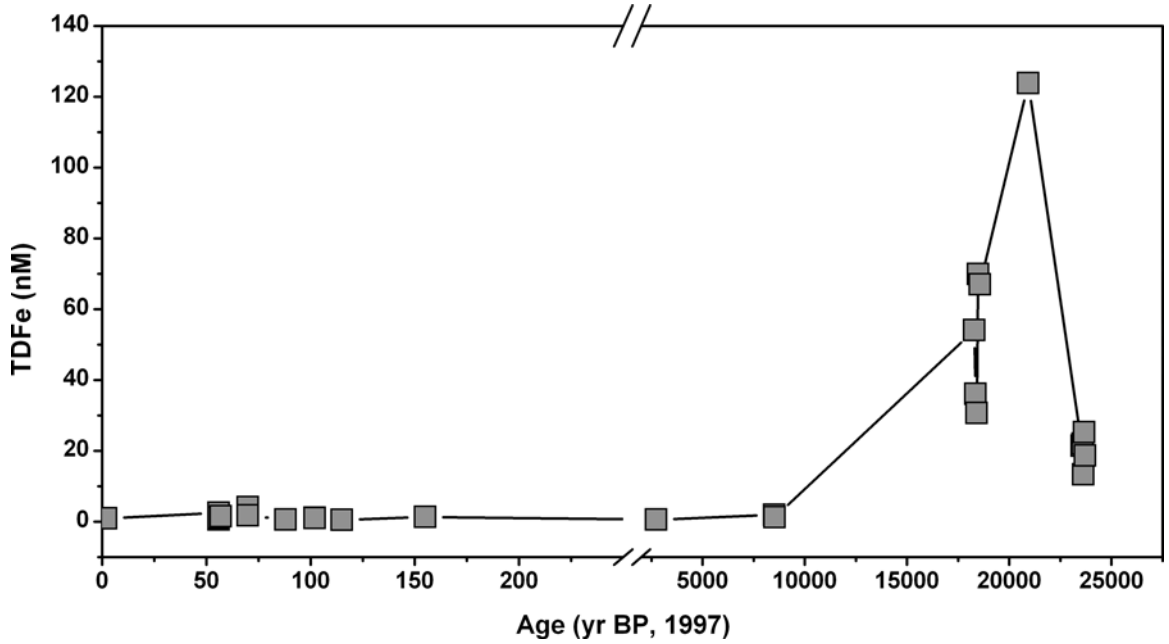

Figure 4. TDFe concentration of all ice core samples versus estimated sample age in years before present (BP, relative to calendar year 1997).

Table 2. Ice Core Total Dissolvable Iron Concentrations

Ice Core	Sample Depth in Core, m	Age in Years Before Present (BP, 1997)	Estimated Time Period Spanned by Core Section	TDFe,[a] nM
DSS	46.64–46.82	56	summer-autumn	2.5
DSS	46.82–46.98	56	winter	0.6
DSS	46.98–47.08	56	spring	1.1
DSS	47.17–47.54	57	summer-autumn	1.4
DSS	72.95–73.20	88	winter	0.5
DSS	895.74–895.99	2,729	~2 yr	0.5
DSS	1106.76–1106.94	8,518	~16 yr	2.0
DSS	1106.94–1107.04	8,530	~10 yr	1.3
DEO8*	0–0.3	1,995	summer	0.9
DEO8	96.01–96.29	69	summer-autumn	4.5
DEO8	96.41–96.55	70	autumn	6.1
DEO8	96.55–96.69	70	winter	1.8
DEO8	136.02–136.16	102	winter	1.0
DEO8	136.16–136.30	102	spring	1.1
DEO8	150.90–151.42	115	winter	0.5
DEO8	192.80–193.08	155	summer	1.3
BHC1	256.28–256.39	18,287	~60 yr	54
BHC1	256.39–256.48	18,345	~60 yr	36
BHC1	256.48–256.59	18,403	~60 yr	31
BHC1	256.59–256.77	18,487	~80 yr	70
BHC1	256.77–256.87	18,568	~80 yr	67
BHC1	262.14–262.28	20,927	~80 yr	124
BHC1	271.76–271.84	23,554	~40 yr	21
BHC1	271.84–271.91	23,591	~40 yr	22
BHC1	271.91–271.99	23,628	~40 yr	13
BHC1	271.99–272.065	23,667	~40 yr	25
BHC1	272.065–272.145	23,705	~40 yr	19

[a] TDFe, total dissolvable iron.

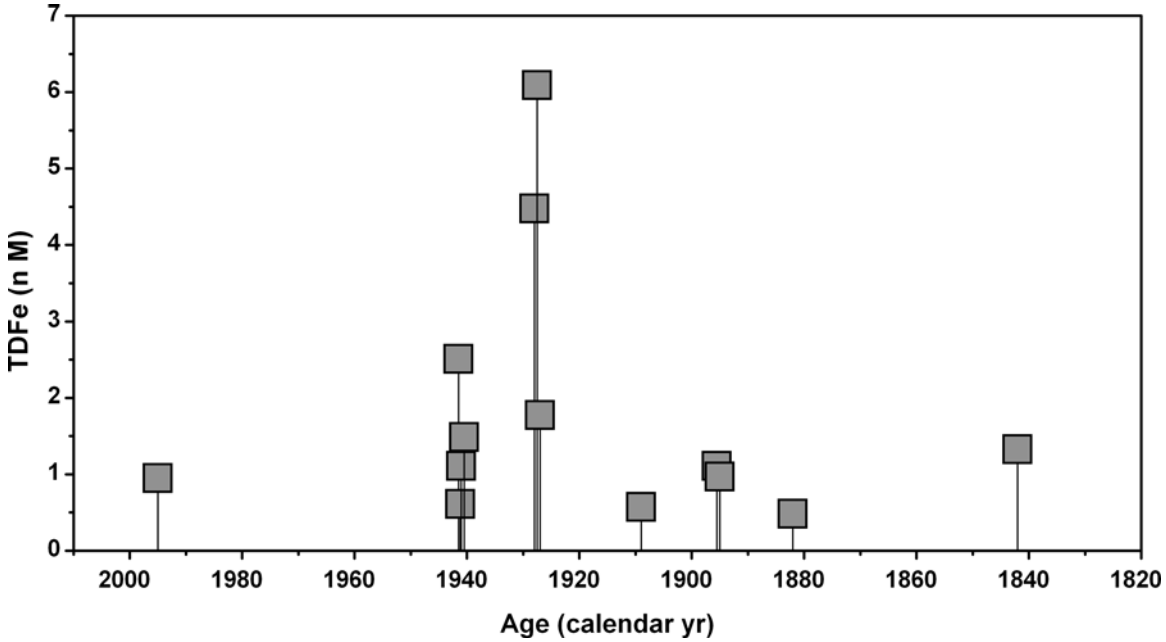

Figure 5. TDFe concentration of Anthropocene ice samples versus age (calendar years).

by dust-transport model simulations of *Mahowald et al.* [1999], by measurements of the isotopic composition of lead in Law Dome ice samples [*Vallelonga et al.*, 2002], and by the recent comparison of Sr and Nd isotopes in Australian dust with previously reported values for East Antarctic ice cores [*Revel-Rolland et al.*, 2006]. If a significant fraction of the soil dust reaching Law Dome is of Australian origin, then this may represent an important contrast between the coastal location of Law Dome and the Antarctic plateau sites of Vostok and Dome C, where dust deposition is thought to be dominated by soils of Patagonian provenance [*Grousset et al.*, 1992; *Basile et al.*, 1997; *Lunt and Valdes*, 2002; *Delmonte et al.*, 2004c]. It is also interesting to note that elevated concentrations of iron or dust particles have been documented in Antarctic ice and firn from Siple Dome in Marie Byrd Land (J. McConnell, personal communication, Desert Research Institute, 2005), from Hercules Nêvê in northern Victoria Land [*Maggi and Petit*, 1998], and from the South Pole [*Boutron and Lorius*, 1979], for samples dating from the period 1928 to 1940. *Maggi and Petit* [1998] proposed that the elevated dust concentrations in Hercules Nêvê firn were associated with low rainfall in South America during the late 1930s. Collectively, these data suggest an enhanced transport of iron-bearing dust to Antarctica during the late 1920s through the 1930s, as a result of drought conditions in Australia and South America.

[14] If we exclude the "anomalous" samples dating from 1927 to 1928, the average TDFe concentration for our Anthropocene- and Holocene-age Law Dome ice samples is 1.2 ± 0.6 nM (n = 14). In contrast, we observed much higher iron concentrations in ice core sections dating from the LD and LGM (Figure 4 and Table 2), with TDFe ranging from 4 nM to 120 nM. Consistent with previous studies of ice cores and marine sediments, the highest Fe concentrations were measured in core sections dating from the LGM, implying elevated levels of mineral dust in the atmosphere during the last glacial epoch. The magnitude and time variation of our TDFe concentration record are in close agreement with the Law Dome dust particle record for the DSS ice core [*Jun et al.*, 1998], and with dust particle records reported for the Vostok and Dome C ice cores [*Petit et al.*, 1999; *Delmonte et al.*, 2004a] (Figure 6). Recent analyses of the EPICA (Dome C) ice core reveal concentrations of "acid-leachable iron" (that measured by ICP-MS after 24 hours acidification to pH 1 with nitric acid) that range from ~5 nM in early Holocene ice to ~320 nM in LGM ice, and concentrations of "total iron" (that measured by ICP-MS after microwave-assisted acid digestion) that range from ~14 nM in early Holocene ice to ~550 nM in LGM ice (estimated from Figure 3 of *Gaspari et al.*

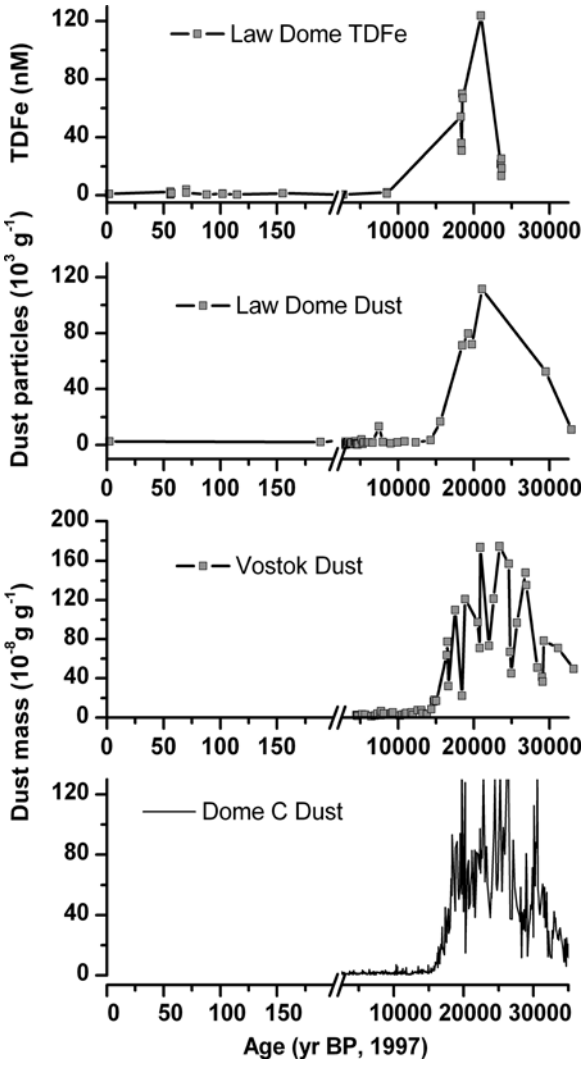

Figure 6. Law Dome TDFe concentrations record in comparison to dust concentration records for ice cores from Law Dome, Vostok, and Dome C (see text).

[2006]). These values are higher than the TDFe concentrations we measured in Law Dome ice of comparable age; however, it is not really useful to compare the iron concentrations of ice from Law Dome and Dome C, because of the much higher ice accumulation rate at Law Dome. Differences in ice accumulation rates are accounted for in the atmospheric flux estimates that are discussed in the following section.

4.2. Estimates of Past Eolian Iron Fluxes

[15] The atmospheric flux of iron to the Law Dome region occurs via both dry and wet deposition. The former can be considered as a relatively continuous process, whereas the latter occurs episodically with precipitation, and is likely to dominate the deposition flux, given the relatively high rates of snow accumulation at Law Dome [*Edwards et al.*, 1998; *Wolff et al.*, 1998, 2006] (Table 1). However, snow accumulation rates in the Law Dome summit region are believed to be relatively constant throughout the year [*Van Ommen and Morgan*, 1997]; thus a significant seasonal bias in wet deposition is considered unlikely. With this assumption, we have calculated an average atmospheric iron deposition flux (which includes both wet and dry deposition) for each core section analyzed, from the product of TDFe concentration and estimated annual ice-accumulation rates (Table 2 and Figure 7). As previously mentioned, the youngest ice core sections used in the study integrate accumulation over periods of less than a year (~1 to 7 months), although we have estimated TDFe deposition fluxes for these samples using annual ice-accumulation rates; thus the fluxes calculated for these samples are the least certain of our deposition estimates.

[16] Table 3 compares the mean value of our estimated eolian iron flux for Law Dome (excluding the anomalous 1927 to 1928 data) to corresponding eolian iron flux estimates for the Dome C and Vostok sites, as calculated from the concentrations of aluminum or dust particles in ice core samples and ice-accumulation rates, assuming that dust has a crustal Al/Fe ratio of 0.841 and contains 3.5% Fe by mass [*Taylor and McClennan*, 1985]. Also shown is a mean estimate of present-day iron deposition in maritime East Antarctica, calculated from measurements of TDFe in modern snow [*Edwards and Sedwick*, 2001], and recently published estimates of atmospheric iron deposition at Dome C during the early Holocene, based on analyses of acid-leachable iron and total iron in the EPICA ice core [*Gaspari et al.*, 2006]. Our mean Holocene TDFe deposition flux estimate for Law Dome of 0.8 μmol m^{-2} yr^{-1} is similar to the estimated deposition flux for present-day maritime East Antarctica (1.1 μmol m^{-2} yr^{-1}), and higher than the iron deposition estimates calculated from aluminum or dust concentrations in the Dome C and Vostok ice cores (0.2–0.6 μmol m^{-2} yr^{-1}). Interestingly, the deposition of acid-leachable iron and total iron estimated by *Gaspari et al.* [2006] for Dome C in the early Holocene (0.13 μmol m^{-2} yr^{-1} and 0.31–0.41 μmol m^{-2} yr^{-1}, respectively) are considerably less than our mean Holocene TDFe deposition estimate for Law Dome. Considered together, the flux estimates in Table 3 imply that atmospheric iron deposition

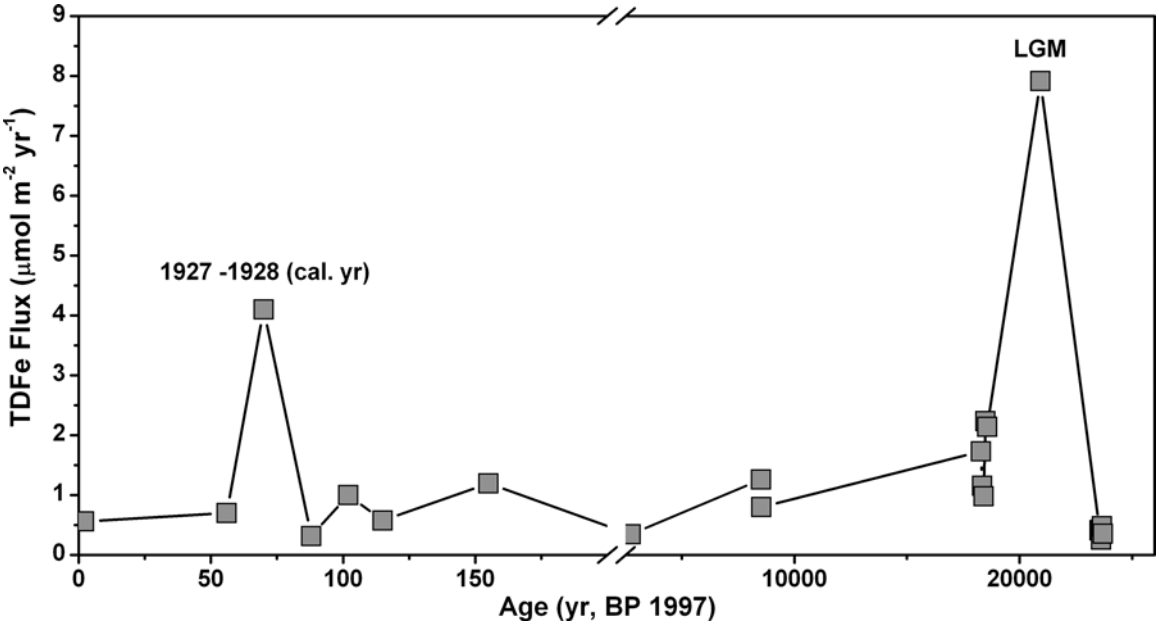

Figure 7. Estimates of eolian TDFe fluxes calculated for all ice core samples versus estimated sample age in years before present (BP, relative to calendar year 1997).

to Law Dome and maritime East Antarctica has been significantly higher than that delivered to Dome C and Vostok during the Holocene.

[17] A possible explanation for this discrepancy lies in the relative ice accumulation rates during the Holocene (Table 3), which are high near the coastal site of Law Dome (~0.8 m H_2O yr^{-1}), but much lower at the inland sites of Dome C and Vostok (~0.02–0.03 m H_2O yr^{-1}). Wet deposition, primarily as snow, has likely dominated the atmospheric flux of iron to coastal sites such as Law Dome during the Holocene, whereas dry deposition has been most important on the inland Antarctic plateau [*Wolff et al.*, 1998, 2006]. Because snow is known to effectively scavenge mineral aerosols from the atmosphere [*Wolff et al.*, 1998], we suggest that wet deposition has maintained an elevated atmospheric iron flux to maritime East Antarctica during the Holocene, relative to inland locations on the Antarctic plateau. Furthermore, this meridional gradient in atmospheric iron depo-

Table 3. Estimates of Average Atmospheric Iron Flux to Antarctica During the Holocene

Site	Reference for Ice Core Data	Data Used	Mean Ice Accum. Rate, m H_2O equiv. yr^{-1}	Reference for Accum. Rate	Estimated Fe Deposition Flux, μmol m^{-2} yr^{-1}
Law Dome	this study	TDFe[a]	0.8[b]	this study	0.8
Maritime East Antarctica	*Edwards and Sedwick* [2001]	TDFe	0.19	*Edwards and Sedwick* [2001]	1.1[c]
Dome C	*Petit et al.* [1981]	Al	0.034	*Lorius* [1989]	0.6
Dome C	*Delmonte et al.* [2004a]	dust	0.025	*Delmonte et al.* [2004a]	0.2
Dome C	*Gaspari et al.* [2006]	ALFe[d] TFe[f]	not given	not given	0.13[e] 0.31–0.41
Vostok	*De Angelis et al.* [1984]	Al	0.023	*Lorius* [1989]	0.4

[a] TDFe, total-dissolvable iron (see text).
[b] Mean net accumulation rate calculated from both DSS and DE08 samples.
[c] Flux was estimated using samples of modern snow.
[d] ALFe, acid-leachable iron (see text).
[e] Early Holocene deposition flux estimated by *Gaspari et al.* [2006]; ice accumulation rates are not provided.
[f] TFe, total iron (see text), here calculated assuming ALFe = 30–40%TFe in Holocene ice [*Gaspari et al.*, 2006].

Table 4. Estimates of Atmospheric Iron Flux to Antarctica During the Last Glacial Maximum

Site	Reference for Ice Core Data	Data Used	Mean Ice Accum. Rate, m H_2O equiv. yr^{-1}	Reference for Accum. Rate	Estimated Fe Deposition Flux, μmol m^{-2} yr^{-1}	Ratio of LGM to Holocene Fe Flux
Law Dome	this study	TDFe[a]	0.07[b]	this study	8	10
Dome C	*Petit et al.* [1981]	Al	0.02	*Lorius* [1989]	7	12
Dome C	*Delmonte et al.* [2004a]	dust	0.01	*Delmonte et al.* [2004a]	5	25
Dome C	*Gaspari et al.* [2006]	ALFe[c]	not given	not given	4.3[d]	33
		TFe[e]			6.6	16–21
Vostok	*De Angelis et al.* [1984]	Al	0.01	*Lorius* [1989]	8	20

[a] TDFe, total-dissolvable iron (see text).
[b] Ice accumulation rate estimated for core BHC1 (see text).
[c] ALFe, acid-leachable iron (see text).
[d] Average LGM deposition flux estimated by *Gaspari et al.* [2006]; ice accumulation rates are not provided.
[e] TFe, total iron (see text), here calculated assuming ALFe = 65%TFe in LGM ice [*Gaspari et al.*, 2006].

sition would have been reinforced by the effect of wet deposition removing aerosol iron from air parcels as they traveled from the Antarctic coast toward the continental interior. Consequently, ice core records from Antarctic plateau sites, such as Dome C, are unlikely to provide quantitative estimates of atmospheric iron deposition to Antarctica waters during the Holocene. In this regard, ice cores from Antarctic coastal locations, such as Law Dome, are likely to provide more useful information.

[18] To calculate atmospheric iron deposition at Law Dome during the LGM and LD (Figure 7), we use the TDFe concentrations measured in sections of the BHC1 ice core and the ice-accumulation rate estimates derived from our proposed age-depth relationship for this core (see section 2.2). We estimate an LGM accumulation rate of 66 kg H_2O m^{-2} yr^{-1} at 20,927 yr before present (BP), which compares well with a recent estimate of 64 kg H_2O m^{-2} yr^{-1} for the ice accumulation rate at the DSS site (Law Dome summit) during the LGM [*Van Ommen et al.*, 2004]. From this, we calculate a maximum TDFe deposition of 8 μmol m^{-2} yr^{-1} during the LGM, a value that is 10 times our average Holocene deposition flux, and in fair to good agreement with estimates of iron deposition for the Dome C and Vostok sites during the LGM (Table 4). The lowest iron deposition estimate for Dome C at the LGM (4.3 μmol m^{-2} yr^{-1}) is that calculated from the acid-leachable iron measurements of *Gaspari et al.* [2006]; this perhaps reflects the incomplete dissolution of acid-labile iron in their meltwater samples, which were acidified for a relatively short period (~24 hours) prior to analysis (compare with Figure 3). For the Law Dome ice core sections from immediately below (age ~23,000 yr BP) and above (age ~18,000 yr BP) our LGM ice, TDFe concentrations are much lower than those in LGM ice, and estimated iron deposition fluxes are similar to our average Holocene TDFe flux estimates (Figure 7). These results are consistent with the rapid variations in dust flux before and after the LGM that have been inferred from analysis of the Vostok and Dome C ice cores [*Petit et al.*, 1999; *Delmonte et al.*, 2004b, 2004c] (Figure 6). The reasonably good agreement between the LGM iron deposition estimates for Law Dome, Dome C, and Vostok suggests that there was less spatial variability in the atmospheric dust flux to East Antarctica during the LGM, relative to the Holocene situation. This probably reflects the much lower ice accumulation rate on the Antarctic coast during the LGM (0.07 m H_2O yr^{-1} at Law Dome, versus 0.8 m H_2O yr^{-1} during the Holocene), hence wet deposition was less important in these areas, and the higher atmospheric dust loadings at this time, which would have been less impacted by precipitation during atmospheric transport.

5. Conclusions

[19] Our data indicate that the atmospheric deposition of total-dissolvable iron to Law Dome and the adjacent Southern Ocean averaged 0.8 μmol m^{-2} yr^{-1} during recent and Holocene times, and was an order of magnitude higher at 8 μmol m^{-2} yr^{-1} during the LGM. These results contrast with recent data from the EPICA Dome C ice core, which suggest that atmospheric deposition of acid-leachable iron during the LGM (4.3 μmol

m^{-2} yr^{-1}) was more than 30-fold higher than the average atmospheric deposition in the early Holocene (0.13 μmol m^{-2} yr^{-1}) [*Gaspari et al.*, 2006; *Wolff et al.*, 2006]. This difference in the LGM/Holocene iron deposition flux ratio between Law Dome and Dome C is largely driven by the higher iron deposition fluxes estimated for Law Dome during the Holocene, which we argue are the result of elevated precipitation over maritime East Antarctica, relative to the Antarctic plateau. Interestingly, these inferred differences in aerosol iron deposition between Law Dome and Dome C are qualitatively consistent with the dust-transport model simulations of *Mahowald et al.* [1999], whose results suggest that there are significant meridional and zonal gradients in the LGM/Holocene dust deposition ratio for the Antarctic region.

[20] A quantitative assessment of the phytoplankton production supported by the iron deposition fluxes we have estimated for the Holocene and the LGM requires additional information that is beyond the scope of this paper, including (1) the fractional solubility and biological availability of the aerosol iron in surface seawater; (2) the role of seasonal sea ice in modulating the delivery of the aerosol iron to the surface ocean; (3) the depth of the ocean surface mixed layer into which the aerosol iron was introduced; and (4) the species composition and Fe/C uptake ratio of the algal community that utilized the aerosol iron [*Martin*, 1990; *Edwards and Sedwick*, 2001; *Bopp et al.*, 2003]. However, within the context of the glacial iron hypothesis, we note that the LGM/Holocene iron flux ratio of ~10 at Law Dome is much less than that considered by *Martin* [1990], who assumed that the atmospheric iron flux to the Southern Ocean at the LGM was 50 times higher than the eolian iron flux during the Holocene.

[21] With regard to the biological availability of aerosol iron, the results of solubility experiments using Antarctic snow suggest that 10 to 90% (geometric mean 32%) of total-dissolvable iron is readily soluble, and presumably available to phytoplankton [*Edwards and Sedwick*, 2001]. Assuming that 32% of the TDFe deposited in the Law Dome region is readily soluble yields deposition fluxes of 0.26 μmol m^{-2} yr^{-1} and 2.6 μmol m^{-2} yr^{-1} for bio-available iron during the Holocene and the LGM, respectively. These values may be compared with the iron fluxes assumed by *Bopp et al.* [2003], who use an ocean biogeochemical model to assess the impact of elevated dust deposition on phytoplankton production during the LGM. These authors prescribe atmospheric iron fluxes based on the modeled dust deposition of *Mahowald et al.* [1999], with the assumption that 0.035% of the dust is soluble iron (hence bio-available). For the ocean region adjacent to Law Dome, this corresponds to bio-available iron fluxes of around 0.6–1.3 μmol m^{-2} yr^{-1} and 1.3–3.1 μmol m^{-2} yr^{-1}, for the present-day and the LGM, respectively. Thus our estimate of the flux of bioavailable iron to the Law Dome region during the Holocene is substantially less than that used in the model simulations of *Bopp et al.* [2003].

[22] One surprising result of our study is the relatively high eolian iron flux estimated for Law Dome during calendar years 1927 and 1928, which we suggest is the result of enhanced dust transport from the drought-affected Australian continent. At 4.1 μmol m^{-2} yr^{-1}, this flux is around half of the eolian iron flux estimated for Law Dome during the LGM. *Karl et al.* [2001] have proposed that decadal-scale changes in eolian iron supply to the subtropical North Pacific have affected significant changes in the algal community structure and biogeochemical cycling of that oceanic region. Given that present-day phytoplankton growth is thought to be limited by iron deficiency over much of the Southern Ocean [*Moore et al.*, 2004], short-term variations in atmospheric iron supply, such as the 1927 to 1928 episode, would be expected to have had a profound impact on the magnitude and nature of primary production over regional scales. The analysis of iron or dust in ice cores at high temporal resolution is required to establish the duration and frequency of such dust transport episodes. In this regard, an increase in the severity of Australian droughts, as is predicted to result from global warming [*Nicholls*, 2004], would be expected to result in an increased transport of aerosol iron to ocean waters in the Australian sector of the Southern Ocean, thus increasing primary production in this region.

[23] The significant discrepancies that exist between eolian iron fluxes estimated from the analysis of ice cores at Law Dome (this study) and Dome C [*Gaspari et al.*, 2006], and from dust transport models [*Mahowald et al.*, 2006] highlight the need for additional ice core records from other Antarctic locations, to better constrain the past deposition of iron to the Southern Ocean. Perhaps the most vexing question concerns the biological availability of eolian iron in the past, given that the preservation of aerosol iron in glacial ice might alter its solubility characteristics over time. Cer-

tainly, it is important to know the fractional solubility of iron in mineral aerosol deposited during the LGM versus that deposited during the Holocene to understand the effects of this atmospheric deposition on ocean biota. Until such information becomes available, the role of eolian iron supply in glacial-interglacial CO_2 changes remains uncertain. As noted by *Martin* [1990], "iron availability appears to have been a player; however, whether it had a lead role or a bit part remains to be determined."

Acknowledgments

[24] The authors gratefully acknowledge the guidance and assistance provided by Ian Allison, Denis Mackey, and Sungmin Hong. Principal funding for this research was provided by the Commonwealth Government of Australia through the Cooperative Research Center for Antarctica and the Southern Ocean.

References

Arimoto, R., R. A. Duce, B. J. Ray, W. G. Ellis, Jr., J. D. Cullen, and J. T. Merrill (1995), Trace elements in the atmosphere over the North Atlantic, *J. Geophys. Res.*, *100*(D1), 1199–1214.

Basile, I., et al. (1997), Patagonian origin of glacial dust deposited in East Antarctica (Vostok and Dome C) during glacial stages 2, 4 and 6, *Earth Planet. Sci. Lett.*, *146*, 573–589.

Bay, R. C., N. Bramall, and P. B. Price (2004), Bipolar correlation of volcanism with millennial climate change, *Proc. Natl. Acad. Sci. U. S. A.*, *101*, 6341–6345.

Blunier, T., and E. J. Brook (2001), Timing of millennial-scale climate change in Antarctica and Greenland during the Last Glacial Period, *Science*, *291*, 109–112.

Bopp, L., K. E. Kohfeld, C. Le Quéré, and O. Aumont (2003), Dust impact on marine biota and atmospheric CO_2 during glacial periods, *Paleoceanography*, *18*(2), 1046, doi:10.1029/2002PA000810.

Boutron, C., and L. Lorius (1979), Trace metals in Antarctic snows since 1914, *Nature*, *277*, 551–554.

Bowie, A. R., P. N. Sedwick, and P. J. Worsfold (2004), Analytical intercomparison between flow injection-chemiluminescence and flow injection-spectrophotometry for the determination of picomolar concentrations of Fe in seawater, *Limnol. Oceanogr. Methods*, *2*, 42–54.

Boyd, P. W., et al. (2000), A mesoscale phytoplankton bloom in the polar Southern Ocean stimulated by iron fertilization, *Nature*, *407*, 695–702.

Broecker, W. S., and G. M. Henderson (1998), The sequence of events surrounding Termination II and their implications for the cause of glacial-interglacial CO_2 changes, *Paleoceanography*, *13*, 353–364.

Brzezinski, M. A., C. J. Pride, V. M. Franck, D. M. Sigman, J. L. Sarmiento, K. Matsumoto, N. Gruber, G. H. Rau, and K. H. Coale (2002), A switch from $Si(OH)_4$ to NO_3^- depletion in the glacial Southern Ocean, *Geophys. Res. Lett.*, *29*(12), 1564, doi:10.1029/2001GL014349.

Candelone, J. P., S. Hong, and C. F. Boutron (1994), An improved method for decontaminating polar snow or ice cores for heavy metal analysis, *Anal. Chim. Acta*, *299*, 9–16.

Coale, K. H., et al. (2004), Southern ocean iron enrichment experiment: Carbon cycling in high- and low-Si waters, *Science*, *304*, 408–414.

Crutzen, P. J., and E. F. Stoermer (2000), The "Anthropocene", *Global Change Newsl.*, *41*, 12–13.

Dai, A., K. E. Trenberth, and T. R. Karl (1998), Global variations in droughts and wet spells: 1900–1995, *Geophys. Res. Lett.*, *25*, 3367–3370.

Dai, A. G., K. E. Trenberth, and T. T. Qian (2004), A global dataset of Palmer Drought Severity Index for 1870–2002: Relationship with soil moisture and effects of surface warming, *J. Hydrometeorol.*, *5*, 1117–1130.

De Angelis, M., et al. (1984), Soluble and insoluble impurities along the 950 m. deep Vostok ice core (Antarctica) climatic implications, *J. Atmos. Chem.*, *1*, 215–239.

De Angelis, M., et al. (1987), Aerosol concentrations over the last climatic cycle (160 Kyr) from an Antarctic ice core, *Nature*, *325*, 318–321.

de Baar, H. J. W., et al. (1995), Importance of iron for plankton blooms and carbon dioxide drawdown in the Southern Ocean, *Nature*, *373*, 412–415.

de Baar, H. J. W., et al. (2005), Synthesis of iron fertilization experiments: From the Iron Age in the Age of Enlightenment, *J. Geophys. Res.*, *110*, C09S16, doi:10.1029/2004JC002601.

Delmonte, B., et al. (2004a), EPICA Dome C Ice Cores Insoluble Dust Data, *Data Contrib. Ser. 2004-040*, http://gcmd.nasa.gov/servlets/md/redirect.py?url=ftp://ftp.ncdc.noaa.gov/pub/data/paleo/icecore/antarctica/epica_domec/edc_dust.txt, IGBP PAGES/World Data Cent. for Paleoclimatol., Boulder, Colo.

Delmonte, B., et al. (2004b), Comparing the Epica and Vostok dust records during the last 220,000 years: Stratigraphical correlation and provenance in glacial periods, *Earth Sci. Rev.*, *66*, 63–87.

Delmonte, B., et al. (2004c), Dust size evidence for opposite regional atmospheric circulation changes over east Antarctica during the last climatic transition, *Clim. Dyn.*, *23*, 427–438.

Donovan, P. (1995), In the interests of the country: A history of the pastoral board of South Australia 1893–1993, South Aust. Dep. of Environ. and Nat. Resour., Openbook, Adelaide, Australia.

Duce, R. A., and N. W. Tindale (1991), Atmospheric transport of iron and its deposition in the ocean, *Limnol. Oceanogr.*, *36*, 1715–1726.

Edwards, R. (2000), Iron in modern and ancient East Antarctic snow: Implications for phytoplankton production in the Southern Ocean, Ph.D. thesis, Univ. of Tasmania, Hobart, Tasmania, Australia.

Edwards, R., and P. Sedwick (2001), Iron in East Antarctic snow: Implications for atmospheric iron deposition and algal production in Antarctic waters, *Geophys. Res. Lett.*, *28*(20), 3907–3910.

Edwards, R., P. N. Sedwick, V. Morgan, C. F. Boutron, and S. Hong (1998), Iron in ice cores from Law Dome, East Antarctica: Implications for past deposition of aerosol iron, *Ann. Glaciol.*, *27*, 365–370.

Etheridge, D. M. (1989), Dynamics of the Law Dome ice cap, as found from bore-hole measurements, *Ann. Glaciol.*, *12*, 46–50.

Etheridge, D. M., G. I. Pearman, and F. de Silva (1988), Atmospheric trace-gas variations as revealed by air trapped in an ice core from Law Dome, Antarctica, *Ann. Glaciol.*, *10*, 28–33.

Fung, I. Y., et al. (2000), Iron supply and demand in the upper ocean, *Global Biogeochem. Cycles*, *14*, 281–295.

Gaspari, V., C. Barbante, G. Cozzi, P. Cescon, C. F. Boutron, P. Gabrielli, G. Capodaglio, C. Ferrari, J. R. Petit, and B. Delmonte (2006), Atmospheric iron fluxes over the last deglaciation: Climatic implications, *Geophys. Res. Lett.*, *33*, L03704, doi:10.1029/2005GL024352.

Grousset, F. E., et al. (1992), Antarctic (Dome C) ice-core dust at 18 Ky BP – Isotopic constraints on origins, *Earth Planet. Sci. Lett.*, *111*, 175–182.

Hamley, T. C., V. I. Morgan, R. J. Thwaites, and X. Q. Gao (1986), An ice-core drilling site at Law Dome summit, Wilkes Land, Antarctica, *ANARE Res. Notes*, *37*, 1–34.

Hesse, P. P., and G. H. McTainsh (1999), Last glacial maximum to early Holocene wind strength in the mid-latitudes of the Southern Hemisphere from aeolian dust in the Tasman Sea, *Quat. Res.*, *52*, 343–349.

Hinkley, T. K., and A. Matsumoto (2001), Atmospheric regime of dust and salt through 75,000 years of Taylor Dome ice core: Refinement by measurement of major, minor, and trace metal suites, *J. Geophys. Res.*, *106*, 18,487–18,493.

Holmes, J., and W. Zoller (1996), The elemental signature of transported Asian dust at Mauna Loa observatory, *Tellus, Ser. B*, *48*, 83–92.

Jickells, T. D., and L. J. Spokes (2001), Atmospheric iron inputs to the oceans, in *The Biogeochemistry of Iron in Seawater*, edited by D. R. Turner and K. Hunter, pp. 85–121, John Wiley, Hoboken, N. J.

Jickells, T. D., et al. (2005), Global iron connections between desert dust, ocean biogeochemistry, and climate, *Science*, *308*, 67–71.

Jun, L., J. Jacka, and V. Morgan (1998), Crystal-size and microparticle record in the ice core from Dome Summit South, Law Dome, East Antarctica, *Ann. Glaciol.*, *27*, 343–348.

Karl, D. M., R. R. Bidigare, and R. M. Letelier (2001), Long-term changes in plankton community structure and productivity in the North Pacific Subtropical Gyre: The domain shift hypothesis, *Deep Sea Res., Part II*, *48*, 1449–1470.

Kumar, N., et al. (1995), Increased biological productivity and export production in the glacial Southern Ocean, *Nature*, *378*, 675–680.

Lefèvre, N., and A. J. Watson (1999), Modeling the geochemical cycle of iron in the oceans and its impact on atmospheric CO_2 concentrations, *Global Biogeochem. Cycles*, *13*, 727–736.

Lorius, C. (1989), Polar ice cores: A record of climatic and environmental changes, in *Global Changes of the Past*, edited by R. S. Bradley, pp. 261–294, Univ. Corp. for Atmos. Res. Off. for Interdisciplinary Earth Stud., Boulder, Colo.

Lunt, D. J., and P. J. Valdes (2002), Dust deposition and provenance at the Last Glacial Maximum and present day, *Geophys. Res. Lett.*, *29*(22), 2085, doi:10.1029/2002GL015656.

Maggi, V., and J. R. Petit (1998), Atmospheric dust concentration record from the Hercules Névé firn core, northern Victoria Land, Antarctica, *Ann. Glaciol.*, *27*, 355–359.

Maher, B. A., and P. F. Dennis (2001), Evidence against dust-mediated control of glacial-interglacial changes in atmospheric CO_2, *Nature*, *411*, 176–180.

Mahowald, N., et al. (1999), Dust sources and deposition during the last glacial maximum and current climate: A comparison of model results with paleodata from ice cores and marine sediments, *J. Geophys. Res.*, *104*, 15,895–15,916.

Mahowald, N. M., A. R. Baker, G. Bergametti, N. Brooks, R. A. Duce, T. D. Jickells, N. Kubilay, J. M. Prospero, and I. Tegen (2005), Atmospheric global dust cycle and iron inputs to the ocean, *Global Biogeochem. Cycles*, *19*, GB4025, doi:10.1029/2004GB002402.

Mahowald, N. M., D. R. Muhs, S. Levis, P. J. Rasch, M. Yoshioka, C. S. Zender, and C. Luo (2006), Change in atmospheric mineral aerosols in response to climate: Last glacial period, preindustrial, modern, and doubled carbon dioxide climates, *J. Geophys. Res.*, *111*, D10202, doi:10.1029/2005JD006653.

Martin, J. H. (1990), Glacial-interglacial CO_2 change: The iron hypothesis, *Paleoceanography*, *5*, 1–13.

Martin, J. H., R. M. Gordon, and S. E. Fitzwater (1990), Iron deficiency limits phytoplankton growth in Antarctic waters, *Global Biogeochem. Cycles*, *4*, 5–12.

Matsumoto, K., J. L. Sarmiento, and M. A. Brzezinski (2002), Silicic acid leakage from the Southern Ocean: A possible explanation for glacial atmospheric pCO_2, *Global Biogeochem. Cycles*, *16*(3), 1031, doi:10.1029/2001GB001442.

Measures, C. I., J. Yuan, and J. A. Resing (1995), Determination of iron in seawater by flow injection analysis using in-line preconcentration and spectrophotometric detection, *Mar. Chem.*, *50*, 1–10.

Morgan, V. (1993), Ice core dating and climatic records, *Artefact*, *16*, 8–11.

Morgan, V. I., and A. P. McCray (1985), Enhanced shear zones in ice flow implications for ice cap modeling and core dating, *ANARE Res. Notes*, *28*, 4–9.

Morgan, V. I., et al. (1997), Site information and initial results from deep ice drilling on Law Dome, Antarctica, *J. Glaciol.*, *43*, 3–10.

Morgan, V., et al. (2002), Relative timing of deglacial climate events in Antarctica and Greenland, *Science*, *297*, 1862–1864.

Moore, J. K., M. R. Abbott, J. G. Richman, and D. M. Nelson (2000), The Southern Ocean at the last glacial maximum: A strong sink for atmospheric carbon dioxide, *Global Biogeochem. Cycles*, *14*, 455–475.

Moore, J. K., S. C. Doney, and K. Lindsay (2004), Upper ocean ecosystem dynamics and iron cycling in a global three-dimensional model, *Global Biogeochem. Cycles*, *18*, GB4028, doi:10.1029/2004GB002220.

Nicholls, N. (2004), The changing nature of Australian droughts, *Clim. Change*, *63*, 323–336.

Petit, J. R., M. Briat, and A. Royer (1981), Ice age aerosol content form East Antarctic ice core samples and past wind strength, *Nature*, *293*, 391–394.

Petit, J. R., et al. (1999), Climate and atmospheric history of the past 420,000 years from the Vostok ice core, Antarctica, *Nature*, *399*, 429–436.

Popova, E. E., V. A. Ryabchenko, and M. J. R. Fasham (2000), Biological pump and vertical mixing in the Southern Ocean: Their impact on atmospheric CO_2, *Global Biogeochem. Cycles*, *14*, 477–498.

Prospero, J. M., P. Ginoux, O. Torres, S. E. Nicholson, and T. E. Gill (2002), Environmental characterization of global sources of atmospheric soil dust identified with the NIMBUS 7 Total Ozone Mapping Spectrometer (TOMS) absorbing aerosol product, *Rev. Geophys.*, *40*(1), 1002, doi:10.1029/2000RG000095.

Rea, D. K. (1994), The paleoclimatic record provided by eolian deposition in the deep sea: The geologic history of wind, *Rev. Geophys.*, *32*(2), 159–196.

Revel-Rolland, M., et al. (2006), Eastern Australia: A possible source of dust in East Antarctica interglacial ice, *Earth Planet. Sci. Lett.*, *249*(1–2), 1–13.

Ridgwell, A. J., and A. J. Watson (2002), Feedback between aeolian dust, climate, and atmospheric CO_2 in glacial time, *Paleoceanography*, *17*(4), 1059, doi:10.1029/2001PA000729.

Ridgwell, A. J., A. J. Watson, and D. E. Archer (2002), Modeling the response of the oceanic Si inventory to perturbation, and consequences for atmospheric CO_2, *Global Biogeochem. Cycles*, *16*(4), 1071, doi:10.1029/2002GB001877.

Rowden-Rich, R. J. M., and C. J. L. Wilson (1996), Models for strain localization in Law Dome, Antarctica, *Ann. Glaciol.*, *23*, 396–401.

Russell-Head, D. S., and W. F. Budd (1979), Ice sheet flow properties derived from bore-hole shear measurements combined with ice core studies, *J. Glaciol.*, *24*(90), 117–130.

Sedwick, P. N., T. M. Church, A. R. Bowie, C. M. Marsay, S. J. Ussher, K. M. Achilles, P. J. Lethaby, R. J. Johnson, M. M. Sarin, and D. J. McGillicuddy (2005), Iron in the Sargasso Sea (Bermuda Atlantic Time-series Study region) during summer: Eolian imprint, spatiotemporal variability, and ecological implications, *Global Biogeochem. Cycles*, *19*, GB4006, doi:10.1029/2004GB002445.

Taylor, S. R., and S. M. McClennan (1985), *The Continental Crust: Its Composition and Evolution*, pp. 66–67, Blackwell Sci., Malden, Mass.

Tegen, I., and I. Fung (1994), Modeling of mineral dust in the atmosphere: Sources, transport, and optical thickness, *J. Geophys. Res.*, *99*(D11), 22,897–22,914.

Townsend, A. T., and R. Edwards (1998), The ultra trace analysis of Antarctic snow and ice samples using high resolution ICP-MS, *J. Anal. At. Spectrom.*, *13*, 463–468.

Traversi, R., et al. (2004), Aluminum and iron record for the last 28 kyr derived from the Antarctic EDC96 ice core using new CFA methods, *Ann. Glaciol.*, *39*, 300–306.

Vallelonga, P., et al. (2002), The lead pollution history of Law Dome, Antarctica, from isotopic measurements on ice cores: 1500 AD to 1989 AD, *Earth Planet. Sci. Lett.*, *204*, 291–306.

Van Ommen, T. D., and V. Morgan (1997), Calibrating the ice core paleothermometer using seasonality, *J. Geophys. Res.*, *102*, 9351–9357.

Van Ommen, T. D., V. Morgan, and M. A. J. Curran (2004), Deglacial and Holocene changes in accumulation at Law Dome, East Antarctica, *Ann. Glaciol.*, *39*, 359–365.

Warren, S. G., and W. J. Wiscombe (1980), A model for the spectral albedo of snow. II. Snow containing atmospheric aerosols, *J. Atmos. Sci.*, *37*, 2734–2745.

Watson, A. J. (1997), Volcanic iron, CO_2, ocean productivity and climate, *Nature*, *385*, 587–588.

Watson, A. J., et al. (2000), Effect of iron supply on Southern Ocean CO_2 uptake and implications for glacial atmospheric CO_2, *Nature*, *407*, 730–733.

Wolff, E. W., et al. (1998), Relationship between chemistry of air, fresh snow and firn cores for aerosol species in coastal Antarctica, *J. Geophys. Res.*, *103*(D9), 11,057–11,070.

Wolff, E. W., et al. (2006), Southern Ocean sea-ice extent, productivity and iron flux over the past eight glacial cycles, *Nature*, *440*, 491–496.

Zoller, W., E. S. Gladney, and R. A. Duce (1974), Atmospheric concentrations and sources of trace metals at the South Pole, *Science*, *183*, 198–200.